articles

molecular pharmaceutics

Biodistribution and Pharmacokinetic Studies of Bone-Targeting *N*-(2-Hydroxypropyl)methacrylamide Copolymer−Alendronate Conjugates

Huaizhong Pan,[†] Monika Sima,[†] Pavla Kopečková,[†,‡] Kuangshi Wu,[†] Songqi Gao,[†] Jihua Liu,[†] Dong Wang,[§] Scott C. Miller,[||] and Jindřich Kopeček*[,†,‡]

Departments of Pharmaceutics & Pharmaceutical Chemistry/CCCD, Bioengineering, and Radiobiology, University of Utah, Salt Lake City, Utah 84112, and Department of Pharmaceutical Sciences, College of Pharmacy, University of Nebraska Medical Center, Omaha, Nebraska 68198

Received January 4, 2008; Revised Manuscript Received March 11, 2008; Accepted April 1, 2008

Abstract: The biodistribution and pharmacokinetics of bone-targeting *N*-(2-hydroxypropyl)-methacrylamide (HPMA) copolymer−alendronate conjugates were evaluated following intravenous administration of radioiodinated conjugates to young healthy BALB/c mice. The synthesis of a polymerizable and cathepsin K cleavable alendronate derivative, *N*-methacryloylglycylglycylprolylnorleucylalendronate, enabled the preparation of HPMA copolymer−alendronate conjugates with varying composition. Using the RAFT (reversible addition−fragmentation chain transfer) polymerization technique, four conjugates with different molecular weight and alendronate content and two control HPMA copolymers (without alendronate) with different molecular weight were prepared. The results of biodistribution studies in mice demonstrated a strong binding capacity of alendronate-targeted HPMA copolymer conjugates to bone. Conjugates with low (1.5 mol%) alendronate content exhibited a similar bone deposition capacity as conjugates containing 8.5 mol % of alendronate. The molecular weight was an important factor in the biodistribution of the HPMA copolymer conjugates. More conjugate structures need to be evaluated, but the data suggest that medium molecular weights (50−100 kDa) might be effective drug carriers for bone delivery.

Keywords: Alendronate; biodistribution; bone targeting; drug delivery; HPMA copolymer; pharmacokinetics

Introduction

Bone is a highly specified form of connective tissue, which provides an internal support system in all vertebrates. It is also the major source of inorganic ions and actively participates in calcium homeostasis in the body. Bone resorption and formation are well balanced and the bone mass is steady for a healthy skeletal system. Disturbances of this balance are a result of bone diseases, such as osteoporosis, arthritis, and Paget's disease. Each year an estimated 1.5 million people suffer an osteoporotic-related fracture; they are costly and become a chronic burden on both individuals and society.[1]

Many therapeutic interventions have been used to treat various bone diseases, especially osteoporosis. These thera-

* Author to whom correspondence should be addressed. Mailing address: University of Utah, Pharmaceutical Chemistry, 30 S 2000 E Rm 201, Salt Lake City, UT 84112. E-mail: Jindrich.Kopecek@utah.edu. Tel: 801 581 7211. Fax: 801 581 7848.

[†] Department of Pharmaceutics & Pharmaceutical Chemistry/CCCD, University of Utah.

[‡] Department of Bioengineering, University of Utah.

[§] University of Nebraska Medical Center.

[||] Department of Radiobiology, University of Utah.

(1) *America's Bone Health: The State of Osteoporosis and Low Bone Mass in Our Nation*; National Osteoporosis Foundation: Washington, DC, 2002; pp 1−16.

10.1021/mp800003u CCC: $40.75
Published on Web 05/28/2008

pies include hormone replacement therapy,[2] selective estrogen-receptor modulators,[3] calcitonin,[4,5] osteoprotegerin,[6] cathepsin K inhibitors,[7] parathyroid hormone,[8] fluoride,[9] strontium ranelate,[10] statins,[11] prostaglandin E series,[12–17] and bone morphogenetic proteins.[18] But most of the therapeutic agents are not bone specific agents; they can interact with some receptors in other organs, which may cause serious problems and obstruct their clinical application.[19,20]

The design of bone targeting drug delivery systems may improve therapeutic efficacy and decrease side effects. Recently, we developed a new bone-targeting system based on HPMA copolymer.[21] Alendronate (a bisphosphonate)[22,23] and D-aspartic acid octapeptide (D-Asp_8)[24,25] were introduced as bone-targeting moieties. Both targeting moieties, when bound to HPMA copolymer or poly(ethylene glycol), could recognize and strongly bind to biomineral surfaces.[21] An in vivo study of the biodistribution of HPMA copolymer−D-Asp_8 conjugates confirmed that the incorporation of D-Asp_8 as bone-targeting moiety could favorably deposit HPMA copolymer conjugates to the entire skeleton. Higher molecular weight of the conjugate enhanced the deposition to bone due to prolonged half-life in circulation, but it weakened the bone selectivity.[26] Finally, the comparison of the fate of HPMA copolymer−D-Asp_8 conjugate with HPMA copolymer−alendronate conjugate following intravenous administration to ovariectomized rats by histological analysis revealed that the D-Asp_8 containing conjugate favorably recognized resorption sites in skeletal tissues, whereas the alendronate containing conjugate directed the delivery system

(2) Lindsay, R. Hormones and bone health in postmenopausal women. *Endocrine* **2004**, *24*, 223–230.
(3) Cranney, A.; Adachi, J. D. Benefit-risk assessment of raloxifene in postmenopausal osteoporosis. *Drug Safety* **2005**, *28*, 721–730.
(4) Okubo, Y.; Bessho, K.; Fujimura, K.; Kusumoto, K.; Ogawa, Y.; Iizuka, T. Effect of elcatonin on osteoinduction by recombinant human bone morphogenetic protein-2. *Biochem. Biophys. Res. Commun.* **2000**, *269*, 317–321.
(5) Farley, J.; Dimai, H. P.; Stilt-Coffing, B.; Farley, P.; Pham, T.; Mohan, S. Calcitonin increases the concentration of insulin-like growth factors in serum-free cultures of human osteoblast-line cells. *Calcif. Tissue Int.* **2000**, *67*, 247–254.
(6) Capparelli, C.; Kostenuik, P. J.; Morony, S.; Starnes, C.; Weimann, B.; Van, G.; Scully, S.; Qi, M.; Lacey, D. L.; Dunstan, C. R. Osteoprotegerin prevents and reverses hypercalcemia in a murine model of humoral hypercalcemia of malignancy. *Cancer Res.* **2000**, *60*, 783–787.
(7) Yamashita, D. S.; Dodds, R. A. Cathepsin K and the design of inhibitors of cathepsin K. *Curr. Pharm. Des.* **2000**, *6*, 1–24.
(8) Lindsay, R.; Nieves, J.; Formica, C.; Henneman, E.; Woelfert, L.; Shen, V.; Dempster, D.; Cosman, F. Randomised controlled study of effect of parathyroid hormone on vertebral-bone mass and fracture incidence among postmenopausal women on oestrogen with osteoporosis. *Lancet* **1997**, *350*, 550–555.
(9) Riggs, B. L.; Hodgson, S. F.; O'Fallon, W. M.; Chao, E. Y.; Wahner, H. W.; Muhs, J. M.; Cedel, S. L.; Melton, L. J., 3rd. Effect of fluoride treatment on the fracture rate in postmenopausal women with osteoporosis. *N. Engl. J. Med.* **1990**, *322*, 802–809.
(10) Meunier, P. J.; Roux, C.; Seeman, E.; Ortolani, S.; Badurski, J. E.; Spector, T. D.; Cannata, J.; Balogh, A.; Lemmel, E. M.; Pors-Nielsen, S.; Rizzoli, R.; Genant, H. K.; Reginster, J. Y. The effects of strontium ranelate on the risk of vertebral fracture in women with postmenopausal osteoporosis. *N. Engl. J. Med.* **2004**, *350*, 459–468.
(11) Mundy, G.; Garrett, R.; Harris, S.; Chan, J.; Chen, D.; Rossini, G.; Boyce, B.; Zhao, M.; Gutierrez, G. Stimulation of bone formation in vitro and in rodents by statins. *Science* **1999**, *286*, 1946–1949.
(12) High, W. B. Effects of orally administered prostaglandin E-2 on cortical bone turnover in adult dogs: a histomorphometric study. *Bone* **1987**, *8*, 363–373.
(13) Jee, W. S.; Mori, S.; Li, X. J.; Chan, S. Prostaglandin E2 enhances cortical bone mass and activates intracortical bone remodeling in intact and ovariectomized female rats. *Bone* **1990**, *11*, 253–266.
(14) Jorgensen, H. R.; Svanholm, H.; Host, A. Bone formation induced in an infant by systemic prostaglandin-E2 administration. *Acta Orthop. Scand.* **1988**, *59*, 464–466.
(15) Marks, S. C., Jr.; Miller, S. Local infusion of prostaglandin E1 stimulates mandibular bone formation in vivo. *J. Oral Pathol* **1988**, *17*, 500–505.
(16) Marks, S. C., Jr.; Miller, S. C. Local delivery of prostaglandin E1 induces periodontal regeneration in adult dogs. *J. Periodontal Res.* **1994**, *29*, 103–108.
(17) Miller, S. C.; Marks, S. C., Jr. Local stimulation of new bone formation by prostaglandin E1: quantitative histomorphometry and comparison of delivery by minipumps and controlled-release pellets. *Bone* **1993**, *14*, 143–151.
(18) Li, R. H.; Wozney, J. M. Delivering on the promise of bone morphogenetic proteins. *Trends Biotechnol.* **2001**, *19*, 255–265.
(19) Rossouw, J. E.; Anderson, G. L.; Prentice, R. L.; LaCroix, A. Z.; Kooperberg, C.; Stefanick, M. L.; Jackson, R. D.; Beresford, S. A.; Howard, B. V.; Johnson, K. C.; Kotchen, J. M.; Ockene, J. Risks and benefits of estrogen plus progestin in healthy postmenopausal women: principal results From the Women's Health Initiative randomized controlled trial. *J. Am. Med. Assoc.* **2002**, *288*, 321–333.
(20) Espie, M.; Daures, J. P.; Chevallier, T.; Mares, P.; Micheletti, M. C.; De Reilhac, P. Breast cancer incidence and hormone replacement therapy: results from the MISSION study, prospective phase. *Gynecol. Endocrinol.* **2007**, *23*, 391–397.
(21) Wang, D.; Miller, S.; Sima, M.; Kopečková, P.; Kopeček, J. Synthesis and evaluation of water-soluble polymeric bone-targeted drug delivery systems. *Bioconjugate Chem.* **2003**, *14*, 853–859.
(22) Gittens, S. A.; Bansal, G.; Zernicke, R. F.; Uludag, H. Designing proteins for bone targeting. *Adv. Drug Delivery Rev.* **2005**, *57*, 1011–1036.
(23) Lin, J. H. Bisphosphonates: a review of their pharmacokinetic properties. *Bone* **1996**, *18*, 75–85.
(24) Wang, D.; Miller, S. C.; Kopečková, P.; Kopeček, J. Bone-targeting macromolecular therapeutics. *Adv. Drug Delivery Rev.* **2005**, *57*, 1049–1076.
(25) Yokogawa, K.; Miya, K.; Sekido, T.; Higashi, Y.; Nomura, M.; Fujisawa, R.; Morito, K.; Masamune, Y.; Waki, Y.; Kasugai, S.; Miyamoto, K. Selective delivery of estradiol to bone by aspartic acid oligopeptide and its effects on ovariectomized mice. *Endocrinology* **2001**, *142*, 1228–1233.
(26) Wang, D.; Sima, M.; Mosley, R. L.; Davda, J. P.; Tietze, N.; Miller, S. C.; Gwilt, P. R.; Kopečková, P.; Kopeček, J. Pharmacokinetic and biodistribution studies of a bone-targeting drug delivery system based on *N*-(2-hydroxypropyl)methacrylamide copolymers. *Mol. Pharmaceutics* **2006**, *3*, 717–725.

to both resorption and formation sites.[27] Atomic force microscopy analysis indicated that these differences could be attributed to the relatively weak binding of D-Asp_8 to apatite, when compared to bisphosphonates, and the different levels of crystallinity of bone apatite at different functional domains of the skeleton.[27]

In addition to serve as targeting moieties, bisphosphonates are also antiresorption agents.[23] Alendronate and risedronate were found to be effective in reducing the risk to both vertebral and nonvertebral fractures.[28] Lin et al.[29–31] as well as Cocquyt et al.[32] have studied the pharmacokinetics of alendronate following intravenous administration in humans and animals. Alendronate was quickly eliminated from plasma, sequestered in the bone, or excreted by the kidney. About half of alendronate dose may deposit to bone. The development of once per month oral dose (ibandronate)[33] or once a year infusion (zolendronic acid)[34] is patient friendly. However, bisphosphonates have some limiting side effects that include diarrhea, nausea, constipation, mild intestinal upset, severely suppressed bone turnover[35] and possibility of development of osteomalacia and progressive osteolytic lesions resulting in lower patient compliance.[36] Attachment of bisphosphonates to water soluble polymers via biodegradable spacers, which can control the biophosphonate release at bone sites, possesses a potential to minimize side effects. In the design presented here, alendronate is bound to the HPMA copolymer via a cathepsin K sensitive spacer.[37] After the conjugate binds to bone, free alendronate can be released by osteoclasts and act as an antiresorption agent. The polymer chain may detach from the bone and be eliminated from the organism. Such conjugates have the potential to be developed as a combination therapy.

Previously, HPMA copolymer−alendronate conjugates were synthesized[21,27] by attachment of alendronate to a HPMA copolymer precursor containing side chains terminated in reactive *p*-nitrophenyl esters in an aqueous environment. Due to a slow rate of the polymeranalogous reaction and relatively fast hydrolysis of *p*-nitrophenyl esters, the yield of the reaction (amount of attached alendronate) was low, alendronate was attached via (enzymatically) noncleavable bonds, and the conjugate contained COOH groups in the side chain (result of *p*-nitrophenyl ester hydrolysis). Here, a new polymerizable alendronate derivative, *N*-methacryloylglycylglycylprolylnorleucylalendronate, was synthesized. Using the RAFT (reversible addition−fragmentation chain transfer) polymerization technique, four HPMA copolymer−alendronate conjugates with different molecular weight and alendronate content and two control HPMA copolymers (without alendronate) with different molecular weight were prepared. The biodistribution and pharmacokinetics of these (radioiodinated) conjugates were studied following intravenous administration to healthy BALB/c mice.

Experimental Section

Materials. Alendronate, methacryloyl chloride, and H-Gly-Gly-OH were purchased from Sigma (St. Louis, MO). HPMA,[38] *N*-methacryloylglycylglycine (MA-Gly-Gly-OH),[39] 5-[3-(methacryloylaminopropyl)thioureidyl]fluorescein (MA-FITC)[40] and *N*-methacryloyltyrosineamide (MA-Tyr-NH_2)[41] were synthesized as described previously. Trithiocarbonate chain transfer agent *S*,*S*′-bis(α,α′-dimethyl-α″-acetic acid)trithio-

(27) Wang, D.; Miller, S. C.; Shlyakhtenko, L. S.; Portillo, A. M.; Liu, X.-M.; Papangkorn, K.; Kopečková, P.; Lyubchenko, Y.; Higuchi, W. I.; Kopeček, J. Osteotropic peptide that differentiates functional domains of the skeleton. *Bioconjugate Chem.* **2007**, *18*, 1375–1378.

(28) Cranney, A.; Tugwell, P.; Wells, G.; Guyatt, G. Meta-analyses of therapies for postmenopausal osteoporosis. I. Systematic reviews of randomized trials in osteoporosis: introduction and methodology. *Endocr. Rev.* **2002**, *23*, 496–507.

(29) Lin, J. H.; Chen, I. W.; Deluna, F. A.; Hichens, M. Renal handling of alendronate in rats. An uncharacterized renal transport system. *Drug Metab. Dispos.* **1992**, *20*, 608–613.

(30) Lin, J. H.; Chen, I. W.; Duggan, D. E. Effects of dose, sex, and age on the disposition of alendronate, a potent antiosteolytic bisphosphonate, in rats. *Drug Metab. Dispos.* **1992**, *20*, 473–478.

(31) Lin, J. H.; Duggan, D. E.; Chen, I. W.; Ellsworth, R. L. Physiological disposition of alendronate, a potent anti-osteolytic bisphosphonate, in laboratory animals. *Drug Metab. Dispos.* **1991**, *19*, 926–932.

(32) Cocquyt, V.; Kline, W. F.; Gertz, B. J.; Van Belle, S. J.; Holland, S. D.; De Smet, M.; Quan, H.; Vyas, K. P.; Zhang, K. E.; De Greve, J.; Porras, A. G. Pharmacokinetics of intravenous alendronate. *J Clin. Pharmacol.* **1999**, *39*, 385–393.

(33) Epstein, S. Ibandronate treatment for osteoporosis: rationale, preclinical, and clinical development of extended dosing regimens. *Curr. Osteoporosis Rep.* **2006**, *4*, 14–20.

(34) Recker, R. R.; Delmas, P. D.; Halse, J.; Reid, I. R.; Boonen, S.; Garcia-Hernandez, P. A.; Supronik, J.; Lewiecki, E. M.; Ochoa, L.; Miller, P.; Hu, H.; Mesenbrink, P.; Hartl, F.; Gasser, J.; Eriksen, E. F. The effects of intravenous zoledronic acid once yearly on bone remodeling and bone structure. *J. Bone Miner. Res.* **2007**. DOI: 10.1359/jbmr.070906.

(35) Odvina, C. V.; Zerwekh, J. E.; Rao, D. S.; Maalouf, N.; Gottschalk, F. A.; Pak, C. Y. Severely suppressed bone turnover: a potential complication of alendronate therapy. *J. Clin. Endocrinol. Metab.* **2005**, *90*, 1294–1301.

(36) Malden, N. J.; Pai, A. Y. Oral bisphosphonate associated osteonecrosis of the jaws: three case reports. *Br. Dent. J.* **2007**, *203*, 93–97.

(37) Pan, H.; Kopečková, P.; Wang, D.; Yang, J.; Miller, S.; Kopeček, J. Water-soluble HPMA copolymer - prostaglandin conjugates containing a cathepsin K sensitive spacer. *J. Drug Targeting* **2006**, *14*, 425–435.

(38) Kopeček, J.; Bažilová, H. Poly[*N*-(2-hydroxypropyl)methacrylamide]−1, Radical polymerization and copolymerization. *Eur. Polym. J.* **1973**, *9*, 7–14.

(39) Rejmanová, P.; Labský, J.; Kopeček, J. Aminolyses of monomeric and polymeric 4-nitrophenyl esters of methacryloylated amino acids. *Makromol. Chem.* **1977**, *178*, 2159–2168.

(40) Omelyanenko, V.; Kopečková, P.; Gentry, C.; Kopeček, J. Targetable HPMA copolymer-adriamycin conjugates. Recognition, internalization, and subcellular fate. *J. Controlled Release* **1998**, *53*, 25–37.

(41) Duncan, R.; Cable, H. C.; Rejmanová, P.; Kopeček, J.; Lloyd, J. B. Tyrosinamide residues enhance pinocytic capture of N-(2-hydroxypropyl)methacrylamide copolymers. *Biochim. Biophys. Acta* **1984**, *799*, 1–8.

carbonate (TTC) was synthesized according to the literature.[42] 2,2′-Azobis[2-(2-imidazolin-2-yl)propane]dihydrochloride (VA-044) was obtained from Wako Chemicals (Richmond, VA). 2-Chlorotrityl chloride resin (100−200 mesh, 1.1 mmol/g), *N*-Fmoc protected amino acids, benzotriazole-1-yl-oxy-tris-pyrrolidino-phosphonium hexafluorophosphate (PyBOP), and *N*-hydroxybenzotriazole (HOBt) were purchased from EMD Biosciences (San Diego, CA). Hydroxyapatite (HA) DNA grade (Bio-Gel HTP Gel) was from Bio-Rad Laboratories (Hercules, CA). All other reagents and solvents were purchased from VWR International (West Chester, PA).

Methods. UV−vis spectra were measured on a Varian Cary 400 Bio UV−visible spectrophotometer. Mass spectra of all synthesized compounds were obtained using a mass spectrometer Voyager-DE (STR Biospectrometry Workstation, PerSeptive Biosystems, Framingham, MA). The molecular weight and molecular weight distribution of polymers were measured on the ÄKTA FPLC system (GE Healthcare, formerly Amersham) equipped with UV and RI detectors using a Superose 6 HR10/30 column with PBS (pH 7.4) as the mobile phase. The average molecular weights were calculated using a calibration with polyHPMA fractions.

A dynamic light scattering method for effective diameter of the conjugates was performed on a Brookhaven BI-200SM goniometer and BI-9000AT digital correlator equipped with a He−Ne laser ($\lambda = 633$ nm) at room temperature in PBS (pH = 7.4).

Synthesis of a Polymerizable Alendronate Derivative, *N*-Methacryloylglycylglycylprolylnorleucylalendronate (MA-Gly-Gly-Pro-Nle-Alendronate; MA-Aln). First, MA-Gly-Gly-Pro-Nle-OH was synthesized using a solid-phase methodology and manual Fmoc/tBu strategy on 2-chlorotrityl chloride resin as described previously.[43] Briefly, protected amino acids Fmoc-Nle-OH, Fmoc-Pro-OH, and MA-Gly-Gly-OH were coupled successively on 2-chlorotrityl chloride resin, and then the product was cleaved from the resin with trifluoroacetic acid/triisopropylsilane/H_2O (95/2.5/2.5), concentrated under vacuum, precipitated into ether and vaccuum-dried. In the next step, MA-Gly-Gly-Pro-Nle-OH (100 mg, 0.24 mmol) and 4,5-dihydrothiazole-2-thiol (33 mg, 0.28 mmol) were dissolved in 2 mL of dimethylformamide (DMF) and cooled to 0 °C. Dicyclohexylcarbodiimide (60 mg, 0.29 mmol) in 1 mL of DMF was added dropwise to the reaction mixture and stirring continued at 4 °C overnight. After the reaction, dicyclohexylurea was removed by filtration, the filtrate was added to alendronate aqueous solution (70 mg, 0.22 mmol, 4 mL) and pH was adjusted to ∼7.4 by $NaHCO_3$ solution. The reaction mixture was stirred overnight at room temperature. The solvent was removed under vacuum using a rotary evaporator, and the residue was redissolved in water and extracted with ethyl acetate 3 times to remove unreacted 4,5-dihydrothiazole-2-thiol. HPLC purification of the product was performed on the Agilent 1100 series HPLC apparatus equipped with a preparative reverse-phase column (Microsorb MV C18 column, 300 Å 5 μm, 250 × 22 mm) and a diode-array detector. A gradient from 100% of buffer A (water containing 0.1% of trifluoroacetic acid) to 90% of buffer B (acetonitrile containing 0.1% of trifluoroacetic acid) in 90 min with a flow rate of 5 mL/min was used. The monomer was detected at 220 nm. Organic solvents were removed under vacuum using a rotary evaporator, and the monomer was isolated from aqueous solution by freeze-drying; yield 83 mg (60.2%). MS (MALDI-TOF, negative charge): $m/z = 640.28$ (M − H).

Table 1. Monomers in Feed and Yield of Copolymerization

conjugate	HPMA (μmol)	MA-Aln (μmol)	MA-Tyr-NH_2 (μmol)	MA-FITC (μmol)	TTC (μmol)	VA-044 (μmol)	yield (%)
C-Hh	1958	162[a]	43.5	3.76	3.97	3.46	97.5
C-Lh	1958	162[a]	43.5	3.76	19.8	17.3	98.6
C-Hl	2381	62[b]	51.1	3.76	3.97	3.46	83.8
C-Ll	2381	62[b]	51.1	3.76	19.8	17.3	95.0
C-H0	2647	0	54.4	3.76	3.97	3.46	95.5
C-L0	2647	0	54.4	3.76	19.8	17.3	91

[a] 7.5 mol%; [b] 2.5 mol%.

Synthesis of HPMA Copolymer−Alendronate Conjugates by RAFT Copolymerization. HPMA, MA-Aln, MA-Tyr-NH_2, MA-FITC, VA-044, and TTC were dissolved in a mixed solvent of water and a small amount of methanol; the total monomer concentration was about 1 M (∼15 wt %). The polymerization mixtures contained 0, 2.5 or 7.5 mol % of MA-Aln. The content of monomers, initiator, and chain transfer agent in feed is listed in Table 1. The solution was bubbled with N_2 for 30 min, sealed and polymerized at 40 °C for 48 h. After polymerization, the conjugates was precipitated into an excess of acetone, washed with acetone 3 times, dialyzed for 1 day (molecular weight cutoff 25 kDa for high molecular weight copolymers and 6−8 kDa for low molecular weight copolymers), and then freeze-dried.

The formation of chromophoric complex between alendronate and Fe^{3+} ions in perchloric acid solution was used to determine the alendronate content by spectrophotometry.[44] Briefly, 0.1 mL of conjugate (concentration 2−10 mg/mL) was mixed with 0.1 mL of 4 mM $FeCl_3$ and 0.8 mL of 0.2 M $HClO_4$ and absorbance at 300 nm was measured against a blank. The calibration curve was prepared using alendronate solutions at a concentration range 0−3 mM.

The conjugates were identified with three-letter abbreviations, e.g., C-Xy, where C is conjugate; X relates to molecular weight (H, high molecular weight; L, low molecular weight); y relates to alendronate content (0, no content; h, high content; l, low content).

(42) Lai, J. T.; Filla, D.; Shea, R. Functional polymers from novel carboxyl-terminated trithiocarbonates as highly efficient RAFT agents. *Macromolecules* **2002**, *35*, 6754–6756.

(43) Pechar, M.; Kopečková, P.; Joss, L.; Kopeček, J. Associative diblock copolymers of poly(ethylene glycol) and coiled-coil peptides. *Macromol. Biosci.* **2002**, *2*, 199–206.

(44) Kuljanin, J.; Jankovic, I.; Nedeljkovic, J.; Prstojevic, D.; Marinkovic, V. Spectrophotometric determination of alendronate in pharmaceutical formulations via complex formation with Fe(III) ions. *J. Pharm. Biomed. Anal.* **2002**, *28*, 1215–1220.

Preparation of ^{125}I-Labeled conjugates. The copolymers were radioiodinated (^{125}I) with a standard chloramine-T assay and purified with Sephadex PD-10 columns. The specific activity of the hot samples was in the range 45−65 μCi/mg.

Hydroxyapatite (HA) Binding Study. Conjugate solutions in PBS (0.5 mL; concentration 1 mg/mL) were incubated with different amounts of HA (1, 2.5, 5, 7.5, 12.5, and 25 mg) for 60 min at room temperature under mild shaking. After centrifugation, 0.4 mL of the supernatant was diluted with 0.6 mL of borate buffer and concentration of nonbound polymer (FITC) was measured by spectrophotometry.

Animal Study. All animal experiments were performed according to the University of Utah IACUC approved protocols. ^{125}I-Labeled HPMA copolymers (2 mg/100 μL saline containing 0.1 μCi per animal) were administered to BALB/c mice (~20 g, 6 mice/group) via tail vein injection.[26] Animals were sacrificed at designated time points, and blood samples were withdrawn via the caudal vena cava. Major organs such as heart, lungs, kidneys, liver, spleen, and long bones (tibia and femur, ×2) were isolated, processed, and counted with a γ counter (Packard, Minaxi γ, Autogamma 5000 series, calibrated with ^{137}Cs, nominally 0.25 μCi). The dose in blood was corrected according to the body weight of the animals.

Pharmacokinetic Analysis. Blood concentration−time profiles for each animal group were evaluated by noncompartmental analysis using WinNonlin software (version 2.1, Pharsight Corporation, Mountain View, CA). The pharmacokinetic parameters were calculated from standard equations using WinNonlin.

Statistical Analysis. The one-way ANOVA test was used to determine the statistical significance of the differences in the organ deposition among the different molecular weights of the conjugates. Student's unpaired *t* test was used to determine the statistical significance of the differences in the organ deposition between targeted and nontargeted HPMA copolymer conjugates of different molecular weights. $p < 0.05$ was considered statistically significant.

Results

Synthesis of Alendronate Containing Monomer. MA-Gly-Gly-Pro-Nle-OH was synthesized using a solid-phase methodology and a manual Fmoc/tBu strategy on a 2-chlorotrityl chloride resin. Then, MA-Gly-Gly-Pro-Nle-OH was reacted with 4,5-dihydrothiazole-2-thiol to form thiazolidine-2-thione (TT) active groups; the reaction with alendronate produced the alendronate containing monomer. The formation of the MA-Gly-Gly-Pro-Nle-TT intermediate was crucial; direct coupling of MA-Gly-Gly-Pro-Nle-OH with alendronate was not successful. *N*-Hydroxysuccinimide and 4-nitrophenol active esters were also used, but alendronate is very hydrophilic and MA-Gly-Gly-Pro-Nle-OH derivatives are hydrophobic. During the coupling reaction, the active esters hydrolyzed to corresponding acids, resulting in low yield of monomer. Compared with other active esters, the TT active groups are relatively stable in water or water/organic mixed solvents, but possess sufficient reactivity toward the amino group in alendronate.[45] By using the TT active amide, the yield of alendronate monomer was acceptable.

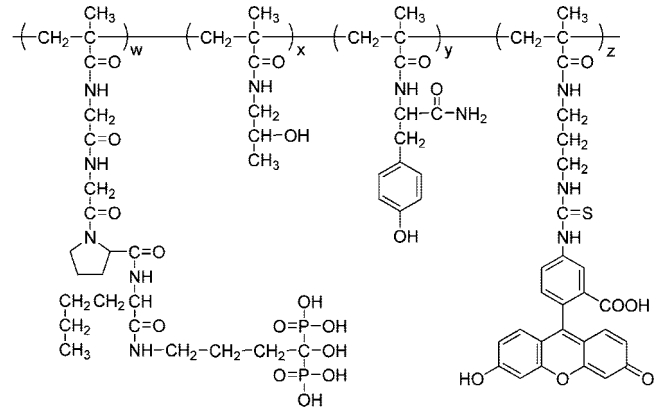

Figure 1. Structure of alendronate containing HPMA copolymer conjugates.

Synthesis of HPMA Copolymer−Alendronate Conjugates. The copolymers were prepared by RAFT copolymerization to achieve control of their molecular weight and polydispersity. Initially, 4,4′-azobis(4-cyanovaleric acid) (V-501) was used as the initiator and 4-cyanopentanoic acid dithiobenzoate as a chain transfer agent (CTA). However, after 24 h at 70 °C, only a 25−27% yield of copolymer was obtained. The reason for the low yield may be a slow hydrolysis of the dithio ester CTA.[46] To improve the polymerization yield, trithiocarbonate was selected as the CTA.[42] Trithiocarbonate CTA is relatively stable under acid and basic conditions. By using VA-044 as a low temperature initiator and *S*,*S*′-bis(α,α′-dimethyl-α″-acetic acid)-trithiocarbonate as the CTA, a high yield of polymer was obtained at 40 °C.

The structure of the conjugates is shown in Figure 1, and the physicochemical characterization of all conjugates used in this study is summarized in Table 2. Three pairs of conjugates differing in molecular weight (low and high) were prepared: zero, low, and high content of alendronate. RAFT polymerization is a versatile controlled/"living" free radical polymerization technique resulting in predetermined molecular weight with narrow polydispersity.[47,48] The molecular weight of polymers can be theoretically calculated by the ratio of monomer concentration to chain transfer agent concentration and the conversion of the polymerization.[46] The molecular weights of the conjugates we synthesized here were calculated around 20 kDa for low molecular weight conjugates and around 100 kDa for high molecular weight

(45) Šubr, V.; Ulbrich, K. Synthesis and properties of new *N*-(2-hydroxypropyl)methacrylamide copolymers containing thiazolidine-2-thione. *React. Funct. Polym.* **2006**, *66*, 1525–1538.

(46) Thomas, D. B.; Convertine, A. J.; Myrick, L. J.; Scales, C. W.; Smith, A. E.; Lowe, A. B.; Vasilieva, Y. A.; Ayres, N.; McCormick, C. L. Kinetics and molecular weight control of the polymerization of acrylamide via RAFT. *Macromolecules* **2004**, *37*, 8941–8950.

Table 2. Physicochemical Characterization of HPMA Copolymer−Alendronate Conjugates

conjugate	M_n[a] (kDa)	M_w[b] (PD[c]) (kDa)	diameter[d] (nm)	Tyr[e] (mol %)	Aln[f] (mol %)	FITC[g] (mol %)
C-L0	18.1	21.5 (1.10)	10.3	1.7	0	0.28
C-Ll	18.9	27.0 (1.13)	12.2	1.4	1.4	0.13
C-Lh	19.8	46.0 (1.30)	18.3	1.2	8.2	0.13
C-H0	94.8	71.4 (1.36)	17.6	1.7	0	0.25
C-Hl	83.4	126.3 (1.49)	23.6	1.5	1.5	0.14
C-Hh	97.4	278.3 (1.80)	49.5	1.3	8.5	0.13

[a] The theoretical molecular weight was calculated according to Thomas et al.[46] [b] Molecular weights were estimated by SEC using PBS (pH 7.4) as the mobile phase. [c] Polydispersity = M_w/M_n. [d] Effective diameter determined by DLS in PBS (pH 7.4), maximum standard deviation ±3.3 nm. [e] Measured by spectroscopy using extinction coefficient for Tyr (295 nm) 2700 M^{-1} cm^{-1} in 1 N NaOH (the background of the polymer was subtracted). [f] Determined by complexation of Aln with Fe^{3+} as described in the *Experimental Section*. [g] Determined using extinction coefficient of MA-FITC 78000 M^{-1} cm^{-1} in 0.1 M borate.

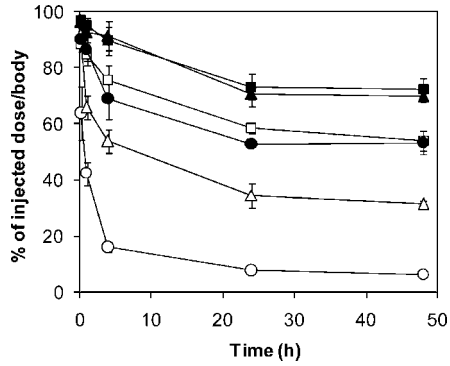

Figure 2. Whole body retention of the HPMA copolymer−alendronate conjugates. Conjugate: ■ C-Hh; ▲ C-Hl; ● C-H0; □ C-Lh; △ C-Ll; ○ C-L0.

conjugates (Table 2). In PBS (same pH as in blood), the size of the conjugates, as determined by dynamic light scattering (Table 2), depended on molecular weight and alendronate content. The latter provides a polyelectrolyte effect; the repulsion of negatively charged alendronate moieties results in an extended conformation of the macromolecules; differences in the extension of conjugate chains, because of slight variation in alendronate content (distribution of chemical composition), results in a mild amplification of the polydispersity of the conjugates. The higher the alendronate content, the larger the molecular size of the conjugates. The effective diameter of the conjugates was in the order of C-Hh > C-Hl > C-H0 ∼ C-Lh > C-Ll > C-L0. The molecular weight estimated by SEC also gave a similar order of apparent molecular weights of the conjugates.

Biodistribution of the Bone-Targeting HPMA Copolymer−Alendronate Conjugates. (a) Retention of the Conjugates in the Organism. Figure 2 illustrates the time profile of the retention of the conjugates in the whole mice. As expected, the elimination of low molecular weight (small molecular size) conjugates from the body is faster than that of the high molecular weight (large molecular size) conjugates. At 48 h, only 6.3% of low molecular weight control C-L0 remained in the organism, whereas for the high molecular weight control, C-H0, 53.3% of the original dose was present. The retention of alendronate containing conjugates correlated with their hydrodynamic volume (effective diameter). At 48 h, the retention of C-Hh and C-Hl conjugates were 72.2% and 69.8% of the original dose, respectively, whereas the retention of C-Lh and C-Ll were 54.1% and 31.4% of the original dose, respectively. The polyelectrolyte effect can be demonstrated by the observation that the retention of low molecular weight conjugate with high alendronate content (C-Lh) was similar to the retention of high molecular weight control polymer, C-H0 (no alendronate). Apparently, the repulsion of negative charges of the alendronate along the copolymer main chain results in the extension of the hydrodynamic volume, so that the molecular size of C-Lh (18.3 nm) was close to that of C-H0 (17.6 nm); see Table 2.

(b) Biodistribution of the Conjugates in Soft Organs. The results of body distribution of HPMA copolymer conjugates and control polymers are shown in Table 3. At 15 min after the administration of the conjugates, the concentrations of all conjugates in the lung and kidney were higher than in heart, liver, and spleen. The distribution of low molecular weight nontargeted control C-L0 in all organs evaluated, except kidney, was transient and declined to very low levels after 4 h.

In heart and lung, the concentrations of all conjugates gradually decreased. The decrease rate showed some molecular weight (size) dependency correlated to the rate of blood clearance (Figure 3). At 24 h, the concentration of the conjugates in the heart and lung was in the order C-Hh ∼ C-Hl > C-H0 ∼ C-Lh > C-Ll > C-L0. At 48 h, the total concentrations were somewhat lower, but the order of conjugates was the same as at 24 h. In kidneys, the concentration of all conjugates gradually decreased with time. The decrease rates of all conjugates were similar regardless of composition. It is interesting to note that the concentration of the low molecular weight control (C-L0) in kidney was always higher than in other organs. One possibility is the reabsorption of a small amount of conjugates in the tubulus after passing through the glomerulus.[49] Due to the fast filtration rate of the low molecular weight conjugate, its reabsorption may be more pronounced.

The accumulation of the conjugates in the liver and spleen depended clearly on molecular weight and alendronate content. For all three pairs of conjugates (zero, low, and high

(47) Convertine, A. J.; Ayres, N.; Scales, C. W.; Lowe, A. B.; McCormick, C. L. Facile, controlled, room-temperature RAFT polymerization of N-isopropylacrylamide. *Biomacromolecules* **2004**, *5*, 1177–1180.

(48) Scales, C. W.; Vasilieva, Y. A.; Convertine, A. J.; Lowe, A. B.; McCormick, C. L. Direct, controlled synthesis of the nonimmunogenic, hydrophilic polymer, poly(N-(2-hydroxypropyl)methacrylamide) via RAFT in aqueous media. *Biomacromolecules* **2005**, *6*, 1846–1850.

(49) Drobník, J.; Rypáček, F. Soluble synthetic polymers in biological systems. *Adv. Polym. Sci.* **1984**, *57*, 1–40.

Table 3. The Biodistribution of the HPMA Copolymer−Alendronate Conjugates with Different Molecular Weights and Alendronate Content[a]

		heart	lung	kidney	liver	spleen	bone
0.25 h	C-L0	2.71 ± 0.35	3.89 ± 0.52	8.17 ± 1.29	1.88 ± 0.28	2.67 ± 0.32	1.53 ± 0.19
	C-Ll	5.81 ± 0.46	7.43 ± 0.27	8.91 ± 0.50	4.81 ± 0.28	4.44 ± 0.33	3.12 ± 0.09
	C-Lh	6.97 ± 0.47	10.96 ± 0.67	9.50 ± 0.24	5.49 ± 0.49	4.87 ± 0.45	3.34 ± 0.13
	C-H0	5.74 ± 0.67	9.38 ± 0.68	9.73 ± 0.36	5.11 ± 0.26	4.55 ± 0.36	2.19 ± 0.10
	C-Hl	6.11 ± 0.86	9.55 ± 1.02	8.70 ± 0.91	6.35 ± 0.63	4.20 ± 0.45	2.43 ± 0.13
	C-Hh	7.41 ± 0.75	11.80 ± 1.03	8.68 ± 0.43	7.61 ± 0.78	5.28 ± 0.49	3.07 ± 0.29
1 h	C-L0	1.81 ± 0.21	2.60 ± 0.19	6.59 ± 0.41	1.30 ± 0.14	2.56 ± 0.29	1.30 ± 0.09
	C-Ll	4.26 ± 0.31	6.21 ± 0.91	7.52 ± 0.22	3.76 ± 0.20	5.84 ± 0.66	3.50 ± 0.34
	C-Lh	6.25 ± 0.37	8.31 ± 0.49	8.18 ± 0.38	4.75 ± 0.20	9.00 ± 0.85	3.62 ± 0.14
	C-H0	6.12 ± 0.44	8.23 ± 0.42	7.48 ± 0.43	4.75 ± 0.42	6.79 ± 1.33	2.91 ± 0.17
	C-Hl	5.36 ± 0.41	6.65 ± 0.84	7.78 ± 0.91	7.42 ± 1.03	6.81 ± 0.94	3.56 ± 0.23
	C-Hh	4.96 ± 1.28	6.01 ± 0.68	7.52 ± 1.82	5.38 ± 1.28	5.65 ± 0.95	3.07 ± 0.14
4 h	C-L0	0.87 ± 0.05	0.96 ± 0.06	5.26 ± 0.26	0.85 ± 0.07	1.04 ± 0.22	0.57 ± 0.06
	C-Ll	3.28 ± 0.36	3.54 ± 0.37	6.05 ± 0.30	2.94 ± 0.21	2.72 ± 0.29	3.59 ± 0.34
	C-Lh	4.53 ± 0.59	5.41 ± 0.45	8.61 ± 0.67	5.27 ± 0.29	4.03 ± 0.27	4.19 ± 0.05
	C-H0	4.93 ± 0.24	5.47 ± 0.28	6.14 ± 0.45	4.06 ± 0.52	3.81 ± 0.48	2.17 ± 0.13
	C-Hl	6.70 ± 0.85	8.56 ± 0.68	8.16 ± 0.64	10.34 ± 0.62	4.60 ± 0.14	3.89 ± 0.13
	C-Hh	7.45 ± 0.88	6.70 ± 0.94	7.07 ± 0.63	5.90 ± 0.37	4.86 ± 0.39	3.77 ± 0.49
12 h	C-L0	0.42 ± 0.03	0.50 ± 0.03	3.03 ± 0.27	0.79 ± 0.07	1.02 ± 0.12	0.34 ± 0.03
	C-Ll	1.68 ± 0.20	2.00 ± 0.15	2.80 ± 0.17	3.23 ± 0.20	3.95 ± 0.35	6.82 ± 0.49
	C-Lh	3.12 ± 0.09	3.90 ± 0.33	3.98 ± 0.22	6.39 ± 0.35	8.35 ± 0.58	6.98 ± 0.49
	C-H0	3.08 ± 0.20	4.20 ± 0.23	3.04 ± 0.04	5.76 ± 0.19	8.37 ± 0.68	2.10 ± 0.13
	C-Hl	3.62 ± 0.22	5.52 ± 0.35	3.74 ± 0.15	8.13 ± 0.30	11.73 ± 0.16	7.04 ± 0.20
	C-Hh	3.81 ± 0.70	5.70 ± 0.38	4.33 ± 0.20	9.17 ± 0.57	13.04 ± 0.88	4.60 ± 0.31
48 h	C-L0	0.38 ± 0.01	0.44 ± 0.02	2.24 ± 0.14	0.67 ± 0.15	0.93 ± 0.05	0.29 ± 0.03
	C-Ll	1.28 ± 0.09	1.33 ± 0.08	2.36 ± 0.15	3.36 ± 0.10	3.84 ± 0.26	7.23 ± 0.25
	C-Lh	2.48 ± 0.16	3.17 ± 0.08	3.43 ± 0.21	7.61 ± 0.38	7.14 ± 0.10	7.80 ± 0.25
	C-H0	2.99 ± 0.18	3.20 ± 0.26	3.03 ± 0.14	6.31 ± 0.20	9.72 ± 0.92	2.08 ± 0.24
	C-Hl	3.16 ± 0.12	4.30 ± 0.25	3.65 ± 0.20	8.36 ± 0.31	12.52 ± 0.39	8.28 ± 0.16
	C-Hh	2.81 ± 0.17	4.31 ± 0.30	4.09 ± 0.27	10.06 ± 0.24	16.15 ± 1.02	5.69 ± 0.33

[a] % of injected dose per gram of tissue.

alendronate content) the higher molecular weight conjugates produced higher deposition. In both organs there was a clear trend of continuing accumulation of high molecular weight conjugates within the 48 h of the experiment. At 24 and 48 h, the concentration of the conjugates in liver and spleen had an order of C-Hh > C-Hl > C-Lh ∼ C-H0 > C-Ll > C-L0.

After 48 h of distribution and clearance, the concentration of alendronate containing conjugates in liver, spleen, and bone were higher than in heart, lung, and kidney. The high molecular weight alendronate containing conjugates (C-Hh and C-Hl) had the highest concentration in the spleen, the concentrations in the liver and bone were similar and the concentrations in heart, lung, and kidney were low. On the other hand, the low molecular weight alendronate containing conjugates (C-Lh and C-Ll) had the highest deposition in bone; their concentration in liver and spleen were similar, and the concentration in heart, lung, and kidney were low. The concentration of control HPMA copolymers (no alendronate) was low in all organs evaluated with two exceptions: the accumulation of conjugate C-L0 in kidney and conjugate C-H0 in liver and spleen were elevated when compared to other organs.

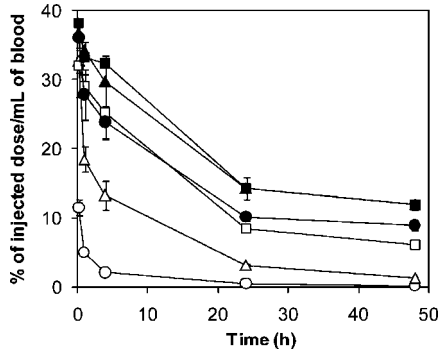

Figure 3. Blood clearance of the HPMA copolymer−alendronate conjugates. Conjugate: ■ C-Hh; ▲ C-Hl; ● C-H0; □ C-Lh; △ C-Ll; ○ C-L0.

(c) Accumulation of the Conjugates in the Skeleton. Table 3 shows the accumulation of the conjugates in the skeleton (represented by tibia and femur). All conjugates reached the skeleton within 15 min after administration. After 1 h, the amount of deposited control conjugates (C-H0 and C-L0) began to decrease. Clearance rate of low molecular weight control C-L0 was faster than that of the high molecular weight control C-H0. Compared with other organs, the concentration of the control conjugates in bone was

Table 4. Pharmacokinetic Parameters of the Conjugates (48 h)

conjugate	AUC (% dose/(mL h))	$T_{1/2(\lambda z)}$ (h)	CL (mL/h)	MRT (h)	V_{ss} (mL)
C-L0	51.4 ± 6.1	12.4 ± 1.4	1.836 ± 0.22	8.8 ± 1.1	17.17 ± 2.2
C-Ll	289.8 ± 27.6	12.4 ± 1.2	0.319 ± 0.03	10.7 ± 1.2	3.70 ± 0.42
C-Lh	622.6 ± 63.1	19.3 ± 2.3	0.126 ± 0.014	14.8 ± 1.6	2.39 ± 0.25
C-H0	673.7 ± 65.3	24.6 ± 2.1	0.101 ± 0.01	17.2 ± 1.5	2.56 ± 0.24
C-Hl	883.0 ± 86.9	28.6 ± 2.6	0.073 ± 0.006	17.9 ± 1.6	2.03 ± 0.18
C-Hh	912.7 ± 89.5	27.7 ± 2.7	0.072 ± 0.007	17.5 ± 1.7	1.92 ± 0.21

always the lowest, apparently due to lack of targeting groups. After 48 h, only 0.29% and 2.08% of original dose of C-L0 and C-H0, respectively, were deposited in the bone. The deposition of alendronate containing conjugates in bone gradually increased with time. Within 24 h, the accumulation of C-Hl, C-Lh and C-Ll in the bone was similar, but higher than C-Hh and much higher than both high molecular weight and low molecular weight controls. After 48 h, the deposition of the conjugates to the bone had an order of C-Hl > C-Lh > C-Ll > C-Hh > C-H0 > C-L0. The results clearly show that, in contrast to nontargeted (no alendronate) controls, alendronate containing conjugates have a tendency of targeting and accumulation to the bone.

Pharmacokinetic Analysis of the Tested Conjugates in Blood. A noncompartmental model was used to evaluate the blood clearance of all conjugates after intravenous administration. The pharmacokinetic parameters for all conjugates are summarized in Table 4. The area under the curve (AUC), terminal elimination half-life ($T_{1/2(\lambda z)}$), clearance (CL), mean residence time (MRT), and apparent volume of distribution at steady-state (V_{ss}) of all conjugates in the blood were molecular size dependent. Conjugates with a small molecular size had a short elimination time, whereas large molecular size conjugates exhibited long elimination times. The $T_{1/2(\lambda z)}$ of the conjugates showed an order of C-Hh ∼ C-Hl > C-H0 > C-Lh > C-Ll > C-L0. The elimination of the conjugates was facilitated primarily by renal filtration. AUC and MRT of the conjugates also increased with increasing of molecular size, while CL and V_{ss} of the conjugates decreased with molecular size. Low V_{ss} of the alendronate containing conjugates reflected that they were restricted in the blood circulation.

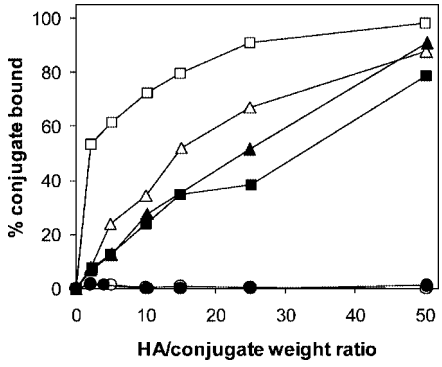

Figure 4. In vitro HA binding ability of HPMA copolymer−alendronate conjugates. ■ C-Hh; ▲ C-Hl; ● C-H0; □ C-Lh; △ C-Ll; ○ C-L0.

Binding of HPMA Copolymer−Alendronate Conjugates to Hydroxyapatite. To demonstrate the direct effect of molecular weight and alendronate content on the binding of the conjugates, the in vitro binding of the conjugates on HA was studied. The results of the in vitro binding of the HPMA copolymer−alendronate conjugates to HA are shown in Figure 4. The efficiency of binding was expressed in % of the original amount of conjugate bound to HA in dependence of the weight ratio HA/conjugate. For low molecular weight conjugates, as expected, a higher content of alendronate (C-Lh) resulted in higher binding than the low alendronate content conjugate (C-Ll). In the case of high molecular weight conjugates, no difference in the binding of high (C-Hh) or low (C-Hl) alendronate content conjugates was observed. Most probably the size of conjugate C-Hh prevented an efficient access to the surface (pores) of HA.

Discussion

HPMA copolymers are intensively studied water-soluble polymeric drug carriers.[50,51] They were mainly evaluated as anticancer drug carriers. A series of recent papers established their potential as carriers of drugs for the treatment of musculoskeletal diseases.[21,26,27,37,52] Two types of bone targeting moieties acting as vectors for water-soluble polymer−drug conjugates have been studied in detail: D-aspartic acid oligopeptides and bisphosphonates. Recently, we discovered that an osteotropic peptide (D-Asp_8) can distinguish between functional domains of the skeleton.[27] The differences in selectivity of binding to bone resorption sites depended on the binding strength. Such an observation has enormous importance for the design of bone-targeted polymeric delivery systems. To enhance targeting efficiency and selectivity, it is possible to incorporate several targeting moieties into one HPMA copolymer macromolecule, thus increasing the apparent binding affinity through multivalent

(50) Kopeček, J. Soluble biomedical polymers. *Polim. Med.* **1977**, *7*, 191–221.

(51) Kopeček, J.; Kopečková, P.; Minko, T.; Lu, Z.-R. HPMA copolymer - anticancer drug conjugates: Design, activity, and mechanism of action. *Eur. J. Pharm. Biopharm.* **2000**, *50*, 61–81.

(52) Hrubý, M.; Etrych, T.; Kučka, J.; Forsterová, M.; Ulbrich, K. Hydroxybisphosphonate-containing polymeric drug-delivery systems designed for targeting into bone tissue. *J. Appl. Polym. Sci.* **2006**, *101*, 3192–3201.

interactions.[53] It appears that the efficacy of a bone-targeted drug delivery system will depend on numerous factors, including the binding strength of the targeting moiety, number of targeting moieties per macromolecule, molecular weight, and conformation of the conjugate in solution. Apparently, the design of an optimal structure will be based on numerous detailed studies.

This contribution aims at obtaining first information on the impact of molecular weight of HPMA copolymer backbone and of the content of alendronate targeting moieties on the body distribution and pharmacokinetics of HPMA copolymer−alendronate conjugates in healthy BALB/c mice. The evaluation of six different structures obviously will not provide a final answer on the structure of the optimal conjugate. Nevertheless, the results will contribute to the understanding of the relationship between the structure of bone-targeted HPMA copolymer conjugates and their fate in organism. In addition, the comparison with previously published data on the biodistribution of HPMA copolymer−D-Asp_8 conjugates[26] will add to our understanding of the targetability of HPMA copolymer based systems to the skeleton.

The biodistribution data obtained support the effective targeting of HPMA copolymer−alendronate conjugates to the bone (Figure 3). The clearance rate of the conjugates from the organism was dependent on molecular size. The concentration of all conjugates gradually decreased with time (Figure 2). One of the most important factors for the clearance of the conjugates obviously was renal filtration; as a part of renal physiology, the kidney can retrieve filtered proteins, peptides, etc. All conjugates may be reabsorbed to some extent. Consequently, small differences in the clearance rate of all conjugates were observed, and the concentration of conjugates in the kidney decreased slowly with time.

The accumulation and clearance of the conjugates in different organs varied. In the heart and the lung, because of large volume of blood passing through these organs, the deposition of the conjugates was largely affected by the blood concentration of the conjugates. After administration, the conjugates accumulated in these organs very fast, followed by a period of continuous decrease. Apparently, due to the absence of a specific ligand, the conjugates did not accumulate in the heart and lung.

In the liver and spleen, with the exception of low molecular weight conjugates, C-L0 and C-Ll, the deposition of all other conjugates increased with time. Due to the presence of sinusoidal blood vessel structures in liver and spleen, and a prolonged intravascular half-life of high molecular weight conjugates, apparently continuous extravasation of such conjugates occurred.

The deposition of nontargeted (control) conjugates, C-H0 and C-L0, to the bone gradually decreased. On the contrary, the alendronate containing conjugates, C-Ll, C-Lh, C-Hl, and C-Hh, continued to accumulate in tibia and femur with time due to the high affinity of alendronate groups to the bone (Table 3). Three conjugates, C-Ll, C-Lh, and C-Hl, deposited similarly without statistically significant differences. But the conjugate C-Hh exhibited the lowest accumulation to the bone within 48 h. This conjugate has a high molecular weight and high alendronate content; it was expected that it would have a high accumulation to the bone. Two phenomena might contribute to this observation (lower binding of C-Hh). The first relates to the molecular size of C-Hh. The effective diameter of C-Hh in PBS (pH 7.4, similar to in blood) was close to 50 nm. Consequently, the rate of extravasation through the fenestrated pore of vasculature in bone may have been impaired resulting in a slower deposition of the conjugate to the bone. The second reason relates to the negative charge of alendronate at physiological conditions. After the polyelectrolyte type macromolecule (with extended conformation) binds to the bone, it will form a shield, which will affect the binding of the conjugate into the porous structure of the bone. To support this hypothesis, we performed an in vitro binding study of the alendronate containing conjugates to HA. An in vitro binding test can avoid physiological effects and only show the result of the molecular weight and alendronate content; this will permit the assessment of the shielding effect (Figure 4). Low molecular weight conjugates exhibited the multivalency effect. The conjugate with higher alendronate content (C-Lh) demonstrated higher deposition to HA than the conjugate C-Ll containing low alendronate content. For high molecular weight alendronate containing conjugates the results were different. Both high alendronate (C-Hh) and low alendronate (C-Hl) containing conjugates bound to HA to a similar extent. In fact, the high alendronate containing conjugate (C-Hh) bound to HA to a slightly lesser extent than conjugate C-Hl (Figure 4). These data are consistent with a shielding effect of high molecular weight and high alendronate containing conjugate (C-Hh) preventing additional conjugate binding into the porous structure of HA. Obviously, in an in vivo situation the results are a combination of binding and clearance of the conjugate. Nevertheless, the shielding effect will be more pronounced with high molecular weight conjugates due to their longer intravascular half-life.

The higher the molecular weight, the longer the retention time of the conjugate in the body or blood; therefore the distribution of the conjugate to all of the organs will increase when compared with low molecular weight compounds. In the presence of targeting groups, here alendronate groups, the biodistribution will change in favor of accumulation of the conjugates at the target site. Increasing the molecular weight, with concomitant prolongation of the retention time, may further enhance the accumulation of the conjugate at the target site. However, a too high molecular weight may also result in a low clearance rate from untargeted organs, shielding effect of charged conjugate, etc. It appears that a suitable molecular weight range for the conjugates needs to be identified.

(53) Tang, A.; Kopečková, P.; Kopeček, J. Binding and cytotoxicity of HPMA copolymer conjugates to lymphocytes mediated by receptor-binding epitopes. *Pharm. Res.* **2003**, *20*, 360–367.

Table 5. Pharmacokinetic Parameters of the HPMA Copolymer Conjugates Containing D-Asp_8 or Alendronate (24 h) Based on Noncompartment Model

conjugate	AUC (% dose/(mL h))	$T_{1/2(\lambda z)}$ (h)	CL (mL/h)	MRT (h)	V_{ss} (mL)
C-L1 (27 kDa)	235.3 ± 24.2	9.3 ± 1.1	0.359 ± 0.03	6.0 ± 0.7	2.6 ± 0.33
D-Asp_8 conjugate (24 kDa)	3.1	5.3	31.0	4.0	130
C-Lh (46 kDa)	446.9 ± 50.1	12.9 ± 1.3	0.165 ± 0.02	7.3 ± 0.8	1.6 ± 0.21
D-Asp_8 conjugate (46 kDa)	63.5	6.4	1.467	4.4	6.9
C-Hl (126 kDa)	568.2 ± 57.3	18.5 ± 1.9	0.105 ± 0.01	8.6 ± 0.9	1.5 ± 0.17
D-Asp_8 conjugate (96 kDa)	405.6	15.3	0.160	8.4	2.1

Comparison of D-Asp_8- and Alendronate-Targeted HPMA Copolymer Conjugates. The results obtained in this study were compared with the biodistribution of HPMA copolymer−D-Asp_8 conjugates (molecular weights 24, 46, and 96 kDa).[26] The distribution trends of both D-Asp_8 containing conjugates[26] and alendronate containing conjugates were similar. At early time intervals after administration, both types of conjugates produced a high deposition to heart, lung, and kidney. The concentration of conjugates in these organs then gradually decreased; after 24 h, the distribution in heart, lung, and kidney was lower than in liver, spleen, and bone. The comparison of bone deposition of D-Asp_8 and alendronate containing HPMA copolymer conjugates showed similar trends in time dependence of deposition, but the amounts deposited to bone differed. HPMA copolymer−D-Asp_8 conjugate (96 kDa) had the highest distribution to bone of all of D-Asp_8[26] and alendronate (this study) containing HPMA copolymer conjugates. However, the deposition of all HPMA copolymer−alendronate conjugates to bone was higher than the deposition of HPMA copolymer−D-Asp_8 conjugates of molecular weights of 24 and 46 kDa. It is important to note that molecular weights for several samples were very similar; apparent molecular weight of C-Ll was 27 kDa and of C-Lh 46 kDa. Apparently, the higher binding affinity of the alendronate group, than that of the D-Asp_8 group, to the bone was responsible. For low molecular weight (size) conjugates, the amount deposited to bone depended on the balance between binding rate and clearance rate. When the molecular size was similar, the high binding affinity of alendronate was decisive for enhanced binding to bone. But for high molecular weight (size) conjugates, the clearance was not the major parameter for binding. The larger molecular size of C-Hl (126.3 kDa) and C-Hh (278.3 kDa) than that of the HPMA copolymer−D-Asp_8 conjugate with molecular weight of 96 kDa may have resulted in an enhanced shielding effect. Consequently, the amount of these HPMA copolymer−alendronate conjugates deposited to bone was lower than that of the 96 kDa HPMA copolymer−D-Asp_8 conjugate.

We further compared the pharmacokinetic parameters (24 h) of alendronate containing conjugates with those of D-Asp_8 containing conjugates using a noncompartment model (Table 5). In spite of similar size of conjugates, the terminal half-lives ($T_{1/2(\lambda z)}$) of the HPMA copolymer−alendronate conjugates were all slightly higher than those of the corresponding HPMA copolymer−D-Asp_8 conjugates, whereas the clearance (CL) and apparent volume of distribution at steady state (V_{ss}) were lower for alendronate containing conjugates than those of the corresponding D-Asp_8 containing conjugates. The pharmacokinetic parameters of HPMA copolymer−D-Asp_8 conjugate (24 kDa) differed from those of the other conjugates. Probably, due to the low molecular weight and high content of D-Asp_8 oligopeptide (∼20 wt % in the conjugate), this conjugate's fate after intravenous administration was similar to that of a small molecular compound (Tyr-D-Asp_8) with a very high clearance rate.[26] Compared with D-Asp_8 containing conjugates, the more negatively charged alendronate groups slow down the blood clearance of HPMA copolymer−alendronate conjugates, especially for lower molecular weight conjugates. The lower V_{ss} values point out that the alendronate containing conjugates were more restricted to the blood circulation and less distributed to other organs than the corresponding D-Asp_8 containing conjugates.

Conclusions

The evaluation of the biodistribution of HPMA copolymer−alendronate conjugates in mice revealed that, due to the high binding affinity for bone, lower alendronate content per macromolecule suffices for good targeting efficacy. Attachment of alendronate groups to HPMA copolymers provides a polyelectrolyte character to the conjugate. The extended conformation of such conjugates will have an impact on the rate of elimination from the organism, deposition to bone, and importantly on the shielding effect resulting in a decrease of conjugate accumulation. More conjugate structures need to be evaluated, but the data suggest that medium molecular weights (50−100 kDa) might be effective drug carriers for bone delivery. Another option, pursued in our laboratory, is the development of high molecular weight polymer carriers containing a degradable bond in the main chain. Such conjugates will possess a long intravascular half-life with concomitant increase in bone accumulation. The carrier deposited in other organs will be eliminated following degradation.

Abbreviations Used

AUC, area under the blood concetration−time curve; C-H0, high molecular weight (control; no alendronate) HPMA copolymer; C-Hh, high molecular weight HPMA copolymer−alendronate conjugate with high alendronate content; C-Hl, high molecular weight HPMA copolymer−

alendronate conjugate with low alendronate content; C-L0, low molecular weight (control; no alendronate) HPMA copolymer; C-Lh, low molecular weight HPMA copolymer−alendronate conjugate with high alendronate content; C-Ll, low molecular weight HPMA copolymer−alendronate conjugate with low alendronate content; CL, clearance; CTA, chain transfer agent; D-Asp_8, D-aspartic acid octapeptide; DLS, dynamic light scattering; DMF, dimethylformamide; HOBt, *N*-hydroxybenzotriazole; HPMA, *N*-(2-hydroxypropyl)methacrylamide; MA-Aln, *N*-methacryloylglycylglycylprolylnorleucylalendronate; MALDI-TOF, matrix assisted laser desorption/ionization time-of-flight; MA-FITC, 5-[3-(methacryloylaminopropyl)thioureidyl]fluorescein; MA-Gly-Gly-OH, *N*-methacryloylglycylglycine; MA-Gly-Gly-Pro-Nle-alendronate, *N*-methacryloylglycylglycylprolylnorleucylalendronate; MA-Gly-Gly-Pro-Nle-OH, *N*-methacryloylglycylglycylprolylnorleucine; MA-Tyr-NH_2, *N*-methacryloyltyrosineamide; MRT, mean residence time; RAFT, reversible addition−fragmentation chain transfer; MS, mass spectrometry; PD, polydispersity; PyBOB, benzotriazole-1-yl-oxy-tris-pyrrolidino-phosphonium hexafluorophosphate; SEC, size exclusion chromatogpraphy; $T_{1/2(\lambda z)}$, terminal elimination half-life; TT, thiazolidine-2-thione active groups; TTC, *S*,*S*′-bis(α,α′-dimethyl-α″-acetic acid)-trithiocarbonate; VA-044, 2,2′-azobis[2-(2-imidazolin-2-yl)propane]dihydrochloride; V_{ss}, apparent volume of distribution at steady state.

Acknowledgment. The research was supported in part by NIH Grants GM069847 (J.K.) and AR053325 (D.W.).

MP800003U